ELSEVIER

Journal of Structural Geology 27 (2005) 871–887

JOURNAL OF STRUCTURAL GEOLOGY

www.elsevier.com/locate/jsg

Geometry and kinematics of adhesive wear in brittle strike-slip fault zones

Mark T. Swanson

Department of Geosciences, University of Southern Maine, Gorham, ME 04038, USA

Received 6 November 2003; received in revised form 12 November 2004; accepted 12 November 2004
Available online 25 April 2005

Abstract

Detailed outcrop surface mapping in Late Paleozoic cataclastic strike-slip faults of coastal Maine shows that asymmetric sidewall ripouts, 0.1–200 m in length, are a significant component of many mapped faults and an important wall rock deformation mechanism during faulting. The geometry of these structures ranges from simple lenses to elongate slabs cut out of the sidewalls of strike-slip faults by a lateral jump of the active zone of slip during adhesion along a section of the main fault. The new irregular trace of the active fault after this jump creates an indenting asperity that is forced to plow through the adjoining wall rock during continued adhesion or be cut off by renewed motion along the main section of the fault. Ripout translation during adhesion sets up the structural asymmetry with trailing extensional and leading contractional ends to the ripout block. The inactive section of the main fault trace at the trailing end can develop a 'sag' or 'half-graben' type geometry due to block movement along the scallop-shaped connecting ramp to the flanking ripout fault. Leading contractional ramps can develop 'thrust' type imbrication and forces the 'humpback' geometry to the ripout slab due to distortion of the inactive main fault surface by ripout translation.

Similar asymmetric ripout geometries are recognized in many other major crustal scale strike-slip fault zones worldwide. Ripout structures in the 5–500 km length range can be found on the Atacama fault system of northern Chile, the Qujiang and Xiaojiang fault zones in western China, the Yalakom–Hozameen fault zone in British Columbia and the San Andreas fault system in southern California. For active crustal-scale faults the surface expression of ripout translation includes a coupled system of extensional trailing ramps as normal oblique-slip faults with pull-apart basin sedimentation and contractional leading ramps as oblique thrust or high angle reverse faults with associated uplift and erosion. The sidewall ripout model, as a mechanism for adhesive wear during fault zone deformation, can be useful in studies of fault zone geometry, kinematics and evolution from outcrop- to crustal-scales.

Keywords: Brittle fault; Fault lens; Strike-slip faulting

1. Introduction

Asymmetric sidewall ripout geometries (Fig. 1) were first reported (Swanson, 1989) from strike-slip fault zones in southern Maine and western Greenland. The association of these ripout geometries with pseudotachylyte in these exposures suggests that friction and flash melting during coseismic slip played an important role during formation of these structures. The plano-convex lens and slab geometry of the sidewall ripouts was attributed to a mechanism of adhesive wear during displacement triggered by lockup along sections of the faults. The adhesion necessary for the development of these structures on the broad range of scales described here, can refer to anything from the loss of melt lubrication during coseismic slip, to an increased resistance to slip associated with changes in rock type or local stress orientations on outcrop-scale structures, or a shift in the pattern of regional seismicity in crustal-scale structures.

This paper offers a new perspective on the structural evolution of sidewall ripouts based on continued detailed mapping in coastal Maine fault zones (Fig. 2) that revealed a complex kinematic history of translation for these structures not considered in the initial ripout paper (Swanson, 1989). Similar ripout structures have also been recognized in several crustal-scale fault zones worldwide. For recently active strike-slip faults ripout translation has developed a distinctive surface morphology expressed as a coupled system of uplift and subsidence on one side of the main fault zone. The recognition of sidewall ripouts with their pattern

E-mail address: mswanson@usm.maine.edu.

0191-8141/$ - see front matter © 2005 Elsevier Ltd. All rights reserved.
doi:10.1016/j.jsg.2004.11.009

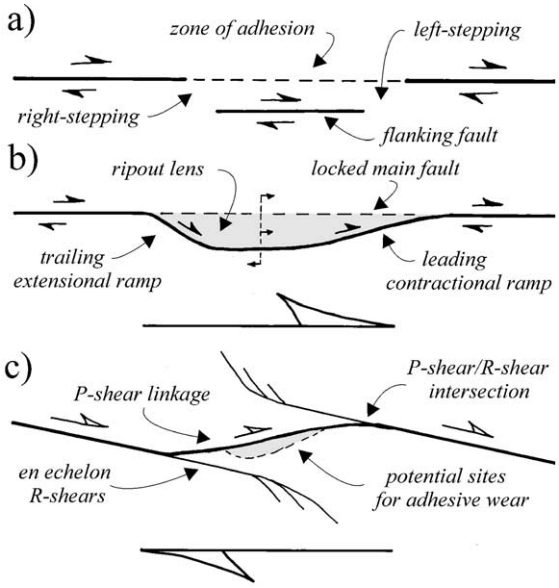

Fig. 1. Geometries of fault lenses, slabs and duplexes attributed to adhesive wear as *sidewall ripouts*. (a) Zone of adhesion on through-going fault surface creates a flanking fault with right- and left-stepping en échelon offsets. (b) Initiation of sidewall ripout links through this double en échelon system with the development of extensional ramps at the trailing edge and contractional ramps at the leading edge of the ripout slab. (c) Restraining steps in en échelon R-shear arrays typically initiate linking P-shears that form an irregular through-going fault with a distinctive restraining bend geometry as a potential site for adhesive wear.

of kinematic development contributes to a more robust interpretive strategy for understanding strike-slip fault zone evolution over a broad range of scales.

1.1. Wear terminology and processes

In the study of friction, the modification of adjacent surfaces during sliding (such as fault walls during displacement) is referred to as *wear* (Rabinowicz, 1965; Bowden and Taber, 1973). Wear has been classified into two types; abrasive wear and adhesive wear. During *abrasive wear,* grinding of one surface against another will scratch and abrade the surfaces, breaking asperity contacts, crushing and grinding the dislocated fragments to create wear debris. In *adhesive wear*, on the other hand, local shear deformation on the microscopic or grain scale causes heating and dynamic welding at asperity contacts. Continued movement can shear around these welded areas and transfer material from one surface to the other during sliding as well as contribute to enhanced abrasive wear. On a more destructive scale in engineering applications, adhesive wear is known as *galling*, *seizing* or *scuffing* and with the removal of flakes of material as *delamination* often leading to mechanical failure (Samuels et al., 1981). Engineering models (Rabinowicz, 1965; Bowman and Stachowiak, 1996; Vingsbo and Hogmark, 1981) show that, in general, adhesive wear processes are enhanced by higher velocities, higher normal stresses and lack of adequate lubrication. Wear fragments in certain engineering examples of adhesive wear are also reported as flake-like with the same wedge-shaped asymmetric geometry (Samuels et al., 1981) as the ripouts described here.

Abrasive wear debris in fault zones is preserved as breccia, gouge, and other cataclasite with varying grain sizes and textures that depend on the displacement history of the fault. Continued displacement promotes the development of finer grained fault zones of sometimes foliated or laminated ultracataclastic debris processed through clast fracturing, grain rotation, grain sliding, cataclastic flow and localized frictional melting. *Adhesive wear* during faulting on the local scale, as described in this paper, results in the cutting out and translation of sections of wall rock (here as the sidewall ripout) due to adhesion or increased resistance to slip along the main fault surface. Where associated with pseudotachylyte, these adhesive wear features may represent a form of 'coseismic scuffing' along the fault zones leaving behind sidewall ripouts as 'earthquake seize marks', borrowing terms from engineering applications.

Fault surface markings, long studied as kinematic indicators for the sense of fault slip (Tija, 1967, 1968, 1971; Hancock and Barka, 1987; Petit, 1987) can also show the local effects of abrasive and adhesive wear. Abrasive wear features include the plow and prod marks made by larger wall rock asperities or angular debris fragments that show as fault striations. Other surface markings such as cuspate or crescentric fractures and chatter marks may represent a plucking action during faulting, possibly due to partial adhesion and wear during sliding. Similar structures are reported from glacially-polished outcrop surfaces produced by ice sliding over bedrock (Riecker, 1965). Of particular note from fault zone studies, Tija (1971) described 'spalling' as a "shallow flaking of the fault surface" and noted that a "steeper wall of lunate fractures rims the lee-side of the depression". Hancock and Barka (1987) also described 'spall marks' resulting from the "local removal of flakes a few cm thick" that were "partly framed by a steep riser which faces down the slip planes". The cross-section geometry described for these spall features shows asymmetry and kinematics similar to the sidewall ripouts discussed here (Fig. 1).

1.2. Asymmetric geometry of sidewall ripouts

Sidewall ripouts in strike slip faults (Fig. 1) as seen in plan view develop as plano-convex fault lenses and slabs where a splay fault diverges away from a section of the main fault trace along a *lateral ramp*. This creates a *flanking fault*, which rejoins the main trace on another lateral ramp farther along strike (Swanson, 1989). The development of the flanking fault creates the right- and left-stepping relations at the ends of the structure that, in turn, control the connecting ramps. This typically creates an asymmetric fault lens that flanks a main fault strand (Fig. 1b). The resulting fault lens geometry is distinctly asymmetric due to the reorientation of stresses at the en échelon steps at either end of the structure,

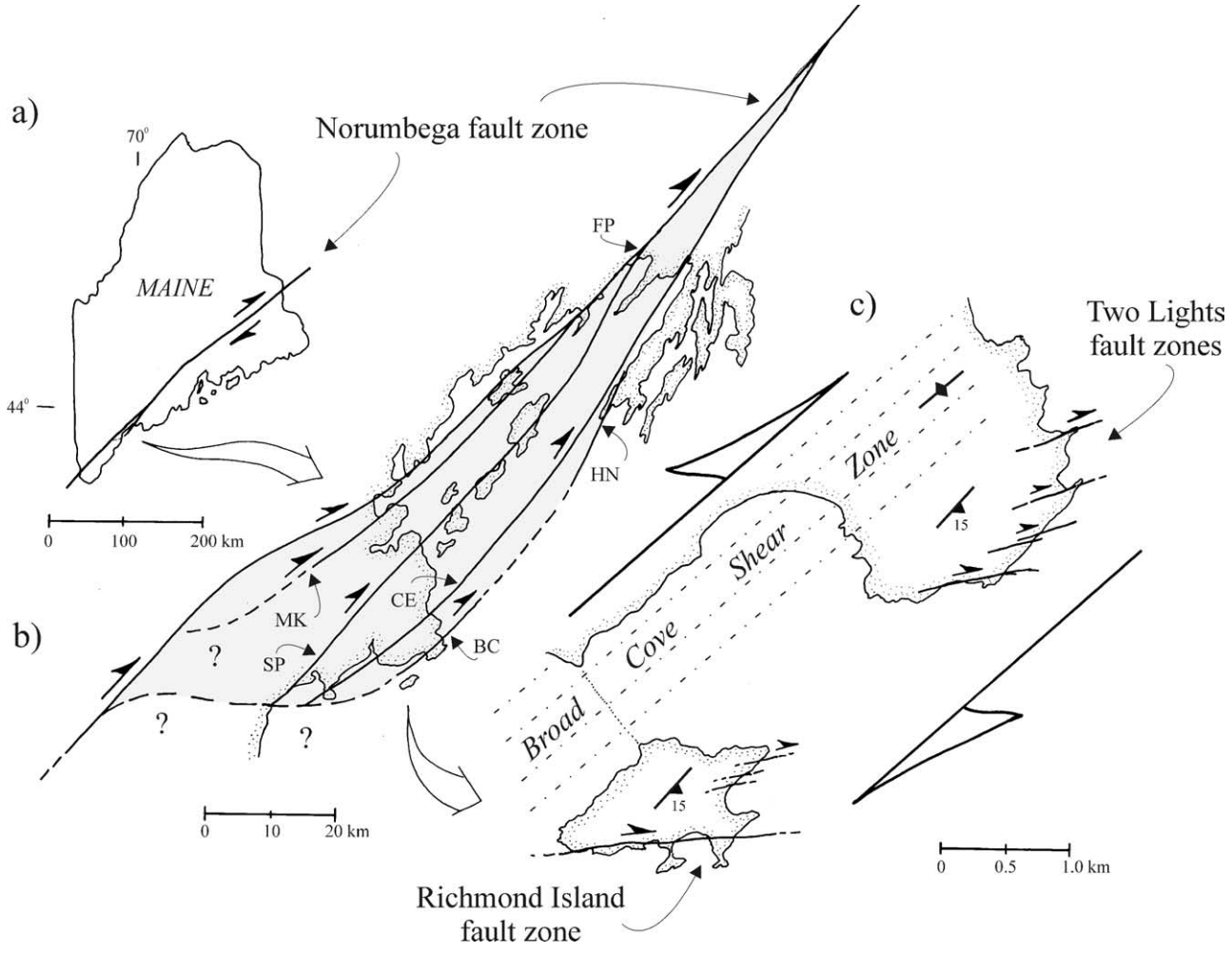

Fig. 2. Location and structural setting of the study area in Cape Elizabeth, Maine. (a) Geometry of the Norumbega fault system through the northern Appalachians and the location of the Casco Bay restraining bend section. (b) Individual fault strands through Casco Bay include the main Flying Point fault zone and several splay faults in a possible ripout geometry. (c) Late brittle strike-slip faults in Cape Elizabeth as the Two Lights and Richmond Island fault zones that flank the steeply-dipping Broad Cove Shear Zone (BC: Broad Cove fault zone; CE: Cape Elizabeth fault; FP: Flying Point fault; HN: Harpswell fault zone; MK: Mackworth fault; SP: South Portland fault).

with listric or scallop-shaped ramps that trail behind the ripout lens during translation with localized fault-parallel extension as the trailing extensional ramp. Slightly oblique splay faults that lead the translation of the ripout lens are formed due to fault-parallel contraction during translation (Fig. 1b) as the leading contractional ramp. This asymmetry allows the use of these ripout geometries as kinematic indicators. Such asymmetry is expected with stress reorientation at linking lateral ramps although pre-existing fabrics and structures can easily influence the orientations of these ramps and the resulting ripout asymmetry. Ripouts are also common in more elongate slab geometries, where fault slip is controlled by planar anisotropies in the host rocks. The common occurrence of pairs of parallel fault segments led to the pseudotachylyte generation zone concept introduced by Grocott (1981), but many of these are likely to have ripout geometries (Swanson, 1989) when examined along strike.

Many lens geometries in fault zones can be attributed to a linkage-growth model for fault zone evolution (Tchalenko, 1970; Bartlett et al., 1981; Naylor et al., 1986). Initial fault arrays of slightly oblique, en échelon R-shears develop P-shear connections (Fig. 1c) to form a through-going fault zone. The restraining orientation of the linking P-shears makes this a potential site for adhesive wear with multiple P-shear linkages that define lenses in a contractional strike-slip duplex (Woodcock and Fischer, 1986). The ripouts, as described here, can also be classified as a type of duplex, but are the result of a double (as opposed to a single) en échelon relationship (Fig. 1a) transferring displacement across a step and then back again to the main fault surface. Similar double en échelon geometry was used in clay model studies of duplex development by Marsh et al. (1990). The leading and trailing ramp structures developed due to ripout lens translation are, in fact, individual strike-slip duplexes (Woodcock and Fischer, 1986; Swanson, 1988) in both extensional and contractional varieties.

1.3. Kinematic development of sidewall ripouts

Sidewall ripouts are interpreted to be the products of adhesive wear (Swanson, 1989), where slabs of wall rock are plucked or ripped out from the sidewall of a main fault by forming a flanking fault during a lateral jump in the active slip surface transferring wall rock from one side of the zone of active faulting to the other. While the main fault section remains in adhesion, the active zone of slip defines an indenting asperity that will plow through the adjoining wall during ripout translation. Continued displacement during adhesion may eventually shear off the ripout/asperity through reactivation of the main fault trace, transferring material back to the other side of the main fault surface. It is the effects of this ripout/asperity translation over a wide range of scales that are considered in this paper.

2. Sidewall ripouts in the Two Lights and Richmond Island fault zones, Maine

New examples of these distinctive asymmetric fault lenses that illustrate the kinematic development of these structures in greater detail were found in the Late Paleozoic cataclastic strike-slip faults in Cape Elizabeth, Maine (Fig. 2). These dextral strike-slip faults are exposed in a coastal terrace of gently dipping Early Paleozoic phyllitic quartzites and include several fault zones (3–5 m displacements) in the Two Lights State Park exposures (numbered from west to east) and one larger fault zone on nearby Richmond Island (40 m displacement). Dextral shearing with very gently-plunging striations and grooves under shallow, brittle crustal conditions as recorded in these cataclastic faults can be correlated with the latest movements of the regional Norumbega dextral strike-slip fault system (Swanson, 1999).

2.1. Hand-sample ripout from the TL-1 fault zone

Locally, the TL-1 fault zone is marked by a well-defined, dark gray, very fine-grained layer only a few millimeters thick made up of a complex mixture of ultracataclasite, foliated cataclasite and pseudotachylyte. A sample of this fault zone was cut into an end-to-end series of three oversize (5×7.5 cm) thin sections (Fig. 3a). The detailed map of this main fault zone (Fig. 3b) was created by on-screen digitizing of thin section features as seen in a high-resolution digital image produced on a flatbed film scanner. This series of thin sections captured a single 15-cm-long ripout structure complete with pseudotachylyte reservoir at the trailing edge and a narrow taper at the leading edge illustrating the typical asymmetric geometry.

2.1.1. Sinistral ripout structure

This ripout and associated pseudotachylyte (Fig. 3b) are the youngest features in the sample, overprinting the main history of dextral displacement. The shear sense based on this asymmetric geometry as well as distinctive offset layers, however, is sinistral as opposed to the dextral shear sense of the overall fault zone. Evidence for dextral shear in these exposures and in these thin sections, such as the oblique orientation of the host rock fabric relative to the fault zone (Fig. 3b), suggests that this antithetic ripout represents a late reversal of slip along the fault zone. The ripout has taken advantage of the planar anisotropy of the host fault zone enhancing the overall slab geometry. Pseudotachylyte occurs as fault-parallel veins and orthogonal injection veins and is preserved in dilatant reservoir structures within both ends of the ripout slab. Sinistral displacement on the flanking ripout fault is $\sim$2 cm (Fig. 3d) while earlier cumulative dextral slip along the main fault zone was $\sim$5 m. The ripout structure has an asymmetric geometry with a leading contractional ramp and an extensional trailing ramp developed due to ripout translation as the ripout/asperity plowed through the adjoining wall rock.

2.1.2. Trailing ramp structures

The slab end rotation associated with the trailing extensional end of the ripout (Fig. 3d) is due to movement of the opposing wall out along the scallop- or listric-shaped ramp to the flanking ripout fault. In the plan view of strike-slip faults this slab end rotation is similar to block rotation and rollover anticlines in cross-section views of listric normal fault systems (e.g. Davis and Reynolds, 1996) although the analogy is purely geometric with no vertical component of movement implied. This block rotation and related fault-parallel extension developed a ‘half-graben’ type offset of the main inactive fault and created a reservoir for cataclasite and friction melt generated by the main slip event. The ‘sag’ geometry of the main fault line may be part of the same translation or represent a second adhesive event. Reactivation along the former line of the main fault cuts this rotated section off and completes the material transfer across the fault, a process inherent to adhesive wear. The geometry of these rotated main fault sections with their ‘half-graben’ and ‘sag’ type geometries, then, suggests ripout translation that contributes to the final ‘humpback’ geometry of the leading edge.

2.1.3. Leading ramp structures

Displacement of the ripout slab for 2 cm while adhering to the main fault has produced the distinctive ‘humpback’ geometry for the leading edge (Fig. 3c). This is due to distortion of the adjacent inactive main fault zone as this wall rock slab rides up along the leading ramp during translation, much like the folding and surface deformation in thin-skinned fold-and-thrust belts (Davis and Reynolds, 1996) although the analogy is purely geometric with no vertical component of movement implied. The main adhesion event probably formed the

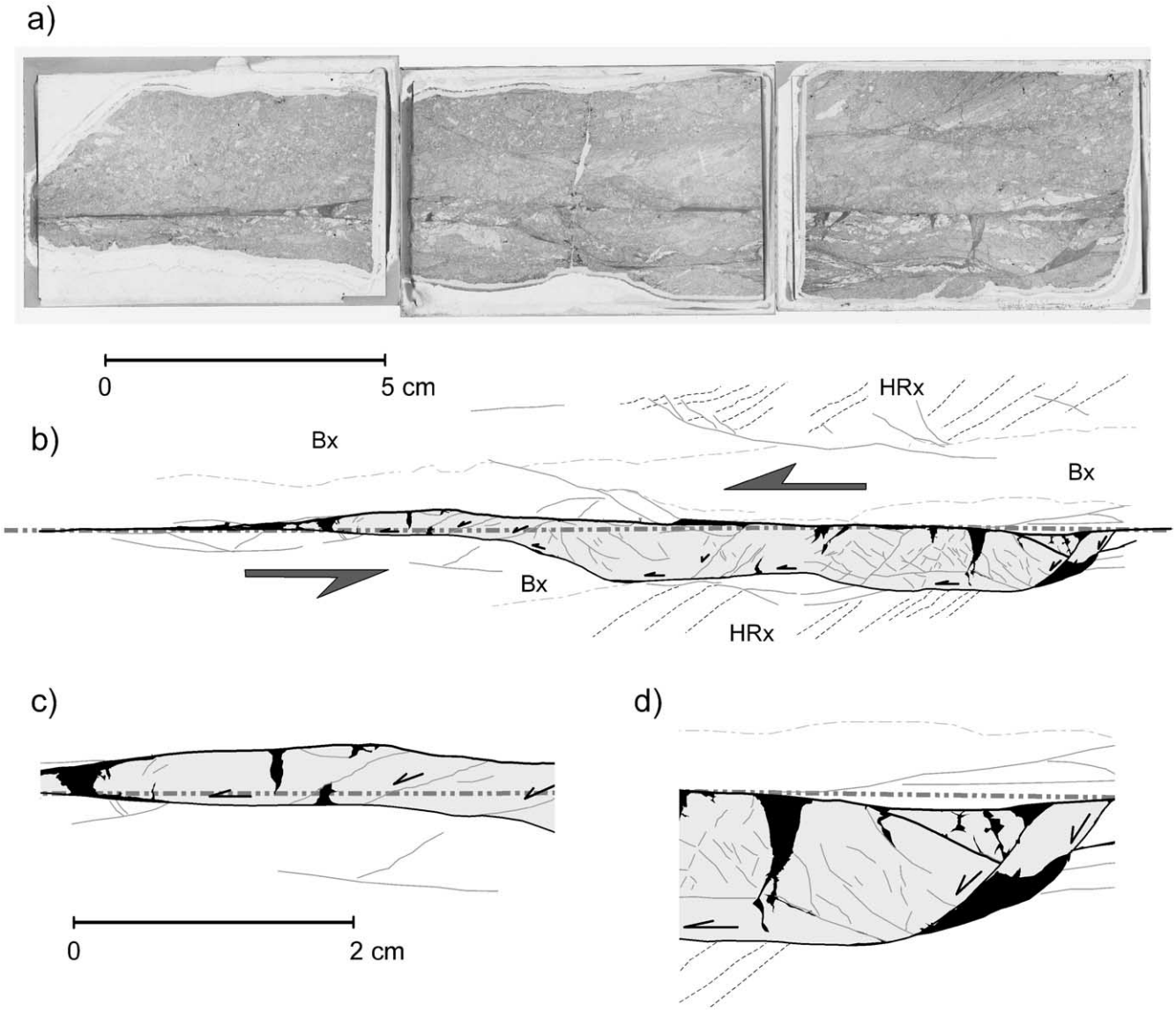

Fig. 3. Detailed structure of the Two Lights hand-sample ripout from three end-to-end oversize (5×7.5 cm) thin sections in a high resolution transmitted light film scan. (a) Digital image of the three-thin-section mosaic. (b) The highlighted structure shows sinistral asymmetry with friction melt reservoir in the extensional trailing end and the humpbacked geometry at the leading end of the ripout slab. Note that the oblique layering in the wall host rock shows the dextral shear sense for the fault zone as opposed to the sinistral shear sense associated with this ripout. (c) Close-up of the leading contractional ramp and humpback geometry of the main fault relative to the original fault line position. (d) Close-up of the trailing extensional ramp with its friction melt reservoir and rotation of the slab end with displacement along the arcuate extensional ramps. The subtle sag geometry of the latest main fault zone relative to a planar reference suggests a second adhesive event (gray = ripout slab; black = pseudotachylyte; Bx = fault zone cataclasites; HRx = host rock metamorphics; black lines = main faults; black dashed lines = host rock layering; gray solid lines = subsidiary faults; dashed gray lines = lithologic boundaries between cataclasite units; heavy gray dashed line = trace of overall fault plane).

'humpback' geometry of the leading edge of the ripout at the same time as the 'half-graben' offset structures in the trailing end of the ripout. Some reactivation of the main fault trace after the first adhesion event is indicated by several late extensional shears found within the leading edge of the slab. The friction melt reservoirs at the leading edge also suggest reactivation with displacements along the main fault trace needed to develop localized pockets of extension along the lee-side of the new 'humpback' obstruction.

2.1.4. Asperity plowing models

The development of adhesion on the main fault, activation of the flanking fault and formation of a ripout lens creates a pronounced asperity geometry to the along-strike shape of the active fault zone. Further displacement along the active fault zone will drive this ripout/asperity through the adjoining wall rock. The plowing of the ripout/asperity can develop accommodation structures within either sidewall due to competence contrast between the host rocks on the two sides of the fault. Two end member

styles for asperity plowing are possible (Fig. 4). Pull-apart structures and 'thrust' type imbrication characterize the 'hard-asperity plowing model' (Fig. 4a), whereas main fault 'sag' or offset in 'half-graben' type geometries and 'hump-humpback' deformation of the main inactive fault section characterize the 'soft-asperity-plowing model' (Fig. 4b). The hand sample ripout just described is an example of the soft-asperity plowing model for ripout translation.

2.2. Outcrop-scale ripout from the TL-1 fault zone

The TL-1 fault zone also hosts an exposure of a 10-m-long ripout structure, 1.5 m wide with inward dipping lateral ramps. This outcrop-scale ripout is localized along a restraining bend in the 600-m-long fault zone exposure. The detailed map of this ripout structure (Fig. 5) was developed using hand-held photo mosaic techniques. The 10-m-long ripout contains three scallop-shaped extensional ramps that converge to a flanking fault and a single ramp at the leading edge. Pseudotachylyte occurs on both the main and flanking ripout faults.

2.2.1. Main fault zone

The N85°E main fault zone alongside the ripout slab consists of multiple fault surfaces that define long slab geometries in a complex anastamosing zone up to 10–15 cm in width (darker gray zone in Fig. 5). A total displacement of ~5 m across the main fault zone is estimated from the 0.4–3.5 m offsets of an early quartz vein cut by at least four separate segments of the main fault. The main fault zone is more complex on the eastern end associated with the leading edge of the ripout with its slight 'humpback' geometry, and is simpler along the western end associated with the trailing end of the ripout and its subtle sag geometry. The hand-sample ripout (depicted in Fig. 3) was collected from the western part of this exposure along the main fault just a few meters beyond the trailing end of this ripout structure.

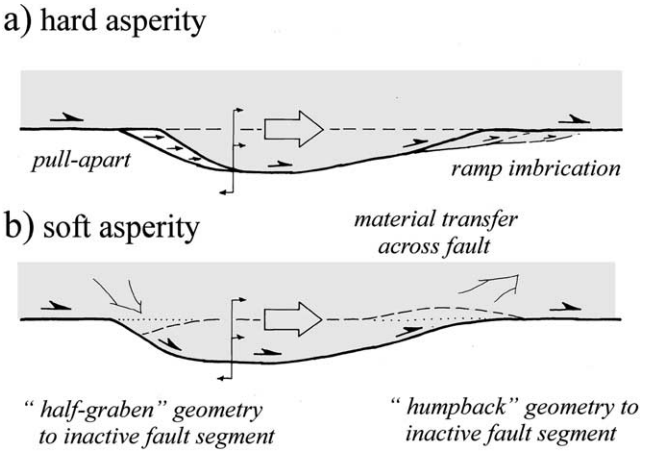

Fig. 4. Asperity plowing models for ripout translation depend on the relative competence of the two sides of the fault. (a) The hard-asperity model with no deformation of the main fault surface. (b) The soft-asperity model with 'half-graben' type offsets and 'humpback' distortions of the main fault surface (arrows = movement at time of adhesion; dashed line = adhering inactive section of main fault trace).

2.2.2. Trailing extensional ramp structures

The trailing ramps leave the main fault at a strike angle of 30–35° and are moderately inclined (37°) toward the ripout. These dipping extensional ramps resemble nested scallops and coalesce to build out the trailing end of the ripout. The last trailing ramp on the western end shows an apparent strike-slip offset of 23 cm and merges with the earlier ramps to yield a 72 cm strike-slip displacement along the flanking fault. Distinctive 'half-graben' type dilatant reservoirs at the trailing ramps similar to structures in the hand sample ripout (Fig. 3) are not evident in this outcrop-scale feature. However, a series of thin lenses may represent a broad, shallow 'sagging' of the main inactive fault section during adhesion and translation followed by cutoff along the now active trace. Such a 'sag cutoff' geometry of the three trailing ramps helps to give this section of the main fault a more open lens structure.

2.2.3. Leading contractional ramp structures

The leading ramp is a simple single surface that strikes at an angle of 35–20° relative to the main fault (Fig. 3) but with a moderate dip towards the ripout of 49° as it approaches the main fault surface. Note the isolated splay off of the leading ramp that turns into en échelon faults suggesting the beginning of imbrication and development of a second leading ramp. The 'humpback' geometry and multiple strands of the main fault zone above the leading ramp suggest repeated fault wall deformation due to ripout translation and development of multiple cutoff faults along the former main fault trace.

2.2.4. Effects of repeated adhesion

Multiple adhesive events that evolve through the translation-cutoff sequence can develop distinctive geometries at the leading (Fig. 6a–f) and trailing (Fig. 6g–l) ends of the ripout structures. Minor ripout translation in a soft-asperity plowing model can lead to the 'sag' geometry for the deformed main fault in the trailing end of the structure (Fig. 6d). More significant ripout translation leads to the offset 'half-graben' type geometry (Fig. 6b) to the inactive main fault. Multiple trailing end structures can be formed by repeated adhesion and reactivation of the main fault (Fig. 6f). In the leading end of the ripout, the 'humpback' cutoff sequences (Fig. 6g–k) can produce an imbricate geometry (Fig. 6l) that, with continued main fault displacements, can be detached and displaced far along the fault zone. This is similar to the development of strike-slip duplexes (Woodcock and Fischer, 1986; Swanson, 1988), but here they occur in linked contractional–extensional pairs along the flanks of strike-slip faults.

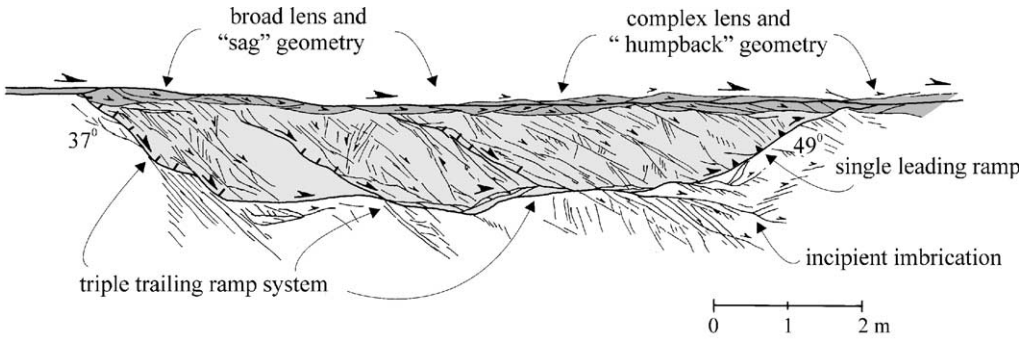

Fig. 5. Detailed photo-mosaic map of the 10-m-long ripout structure (10 m × 1 m) from the restraining bend section of the TL-1 fault zone, Cape Elizabeth, Maine. The trailing extensional end consists of three scallop-shaped moderately-dipping normal oblique-slip surfaces, while the leading contractional end consists of a single oblique-slip thrust surface. Dip angles for leading and trailing ramps as indicated. The gray tone indicates the ripout slab and the darker gray tone highlights the complex main fault zone.

2.3. Outcrop-scale ripout structures from the Richmond Island fault zone

Richmond Island, 2 km offshore from the Two Lights exposures of Cape Elizabeth, hosts a larger 400-m-long fault zone, a wider and more complex fault that accommodated ~40 m of displacement (Fig. 7). Mapping efforts utilized the plane table and alidade at a scale of 1:120 followed by detailing at the outcrop surface. The dominant through-going anastomosing fault zone developed an 80-m-wide linkage duplex (Fig. 7a) between overlapping initial segments. The faults show evidence of brecciation, cataclastic flow and development of ultracataclastic zones up to tens of centimeters wide. Ripouts are common throughout as a significant component of the overall fault structure. Pseudotachylyte is rare.

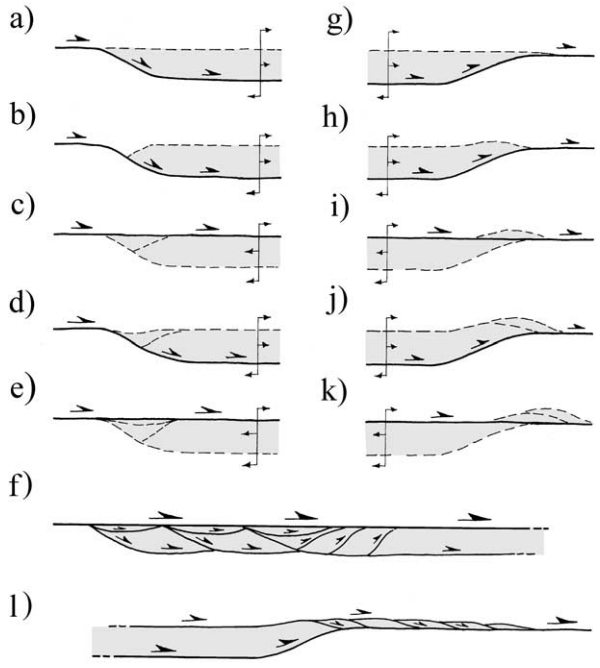

Fig. 6. Effects of repeated adhesion and reactivation on the geometry of the trailing ((a)–(f)) and leading ((g)–(l)) ends of the ripout structures. The trailing structures include the 'sag' and 'half-graben' type main fault deformation. The leading end develops the humpback-cutoff sequence and results in a possible imbricate fault structure (dashed lines represent inactive fault sections).

2.3.1. Ripout geometry and distribution

The fault zone as a whole exhibits an initial en échelon geometry of dextral R-shears with connecting P-shear linkages (Figs. 1c and 7a) and illustrates the linkage-growth model for fault zone evolution. Multiple P-shear linkages within the array develop imbricate contractional strike-slip duplexes (after Woodcock and Fischer, 1986), as seen in Fig. 7b and c. The larger linkage duplex has developed a complex lens structure along the dominant connecting P-shear ramp (Fig. 7a). The restraining orientation of this and other linking segments would promote adhesion and ripout development in accommodating continued displacement. Elongate slab geometries are typical for these ripouts and can be up to 20–25 m long and typically 1–2 m wide (Fig. 7f and g). Multiple ripouts on opposite sides or nested ripouts on the same side occur, suggesting repeated adhesion at the same section of the fault. Multiple trailing extensional ramps are also common with as many as six individual faults, in a cascade of scallop-shaped splays from the main fault trace (Fig. 7f and g).

2.3.2. Corner modification

A much larger ripout (Fig. 7d) is interpreted along the northern section of the main fault zone that is nearly 200 m long and 10 m wide, which cuts through the corner structure created by the P-shear/R-shear intersection within the initial array. Such a corner-cutoff mechanism cuts through the jagged trace of the through-going fault formed by the development of the P-shear linkages. Adhesive wear at these restraining bends can localize along the P-shear segment building out successive imbricate lenses, or along the R-shear segment of the initial en échelon array. The Richmond Island fault structure may reflect a combination of the two, effectively smoothing the corner profile of the through-going linked fault zone.

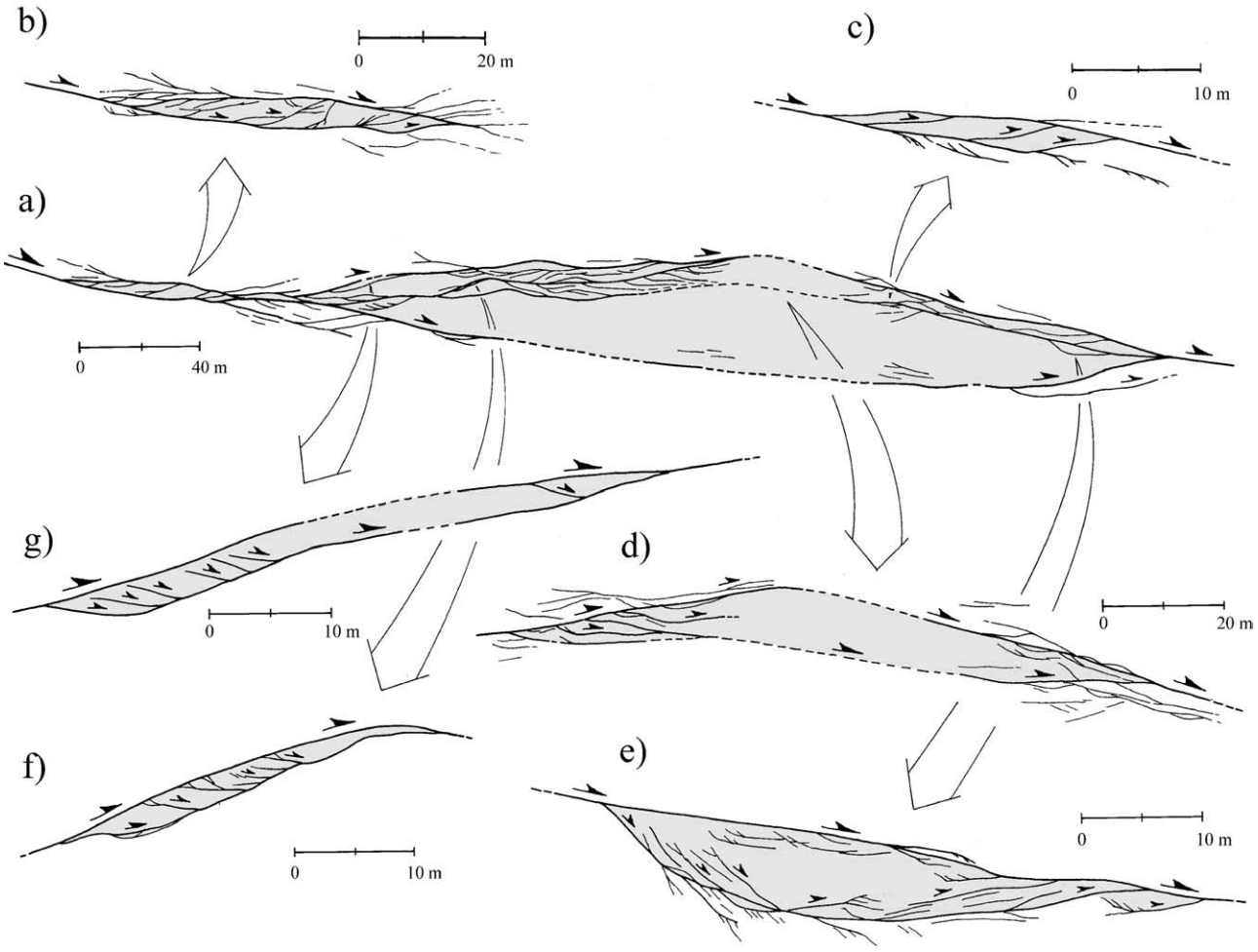

Fig. 7. Distribution and structure of fault lenses within the Richmond Island fault zone, Cape Elizabeth, Maine, clockwise from (a), showing the linkage duplex nature of (a) the entire fault zone exposure and (b) and (c) smaller-scale linkage duplexes, and the nature and distribution of sidewall ripouts, as (f) and (g) along the linking P-shear segments and (d) and (e) along the earlier R-shear segments. (Dashed lines where obscured by seaweed).

3. Ripout structures worldwide

The ripout style of wall rock deformation associated with strike-slip faulting in the coastal Maine exposures also appears to occur on a broader range of scales in many continental strike-slip fault zones worldwide. Recognized ripouts include crustal-scale structures, 5–50 km long, from the Atacama and Domeyko fault systems of western South America (Brown et al., 1993; Reijs and McClay, 1998; Taylor et al., 1998; Arriagada et al., 2000) and the Teletsk shear zone of central Asia (Theunnissen et al., 2002). Outcrop-scale structures associated with pseudotachylyte have been reported in the Gole Larghe fault zone of the southern Italian Alps (DiToro and Pennachioni, 2005). Footwall ripouts were also used as kinematic indicators on the Roche Forte Thrust fault in Portugal (Curtis, 1999) and described as a master fault with a 'rejoining' splay (Walsh et al., 1999). Ripouts were also included in a summary diagram for strike-slip tectonics (Woodcock and Schubert, 1995), where they are mentioned in reference to horses, shear lenses and strike-slip duplexes. Previously unrecognized ripout structures from North America and Asia are described below.

3.1. The Yalakom–Hozameen fault system, British Columbia–Washington

An excellent example of this structure at a crustal scale occurs at a restraining bend on the dextral Yalakom fault system of British Columbia, expressed as a ripout lens, ~500 km long and 25 km wide (Fig. 8). Mapping of the Yalakom fault system was conducted by Umhoefer and Kleinspehn (1995) and Umhoefer and Schiarizza (1996), who reported on the fault system in two different papers, one focused on the northwestern section (Umhoefer and Kleinspehn, 1995), the trailing extensional end of the ripout structure, and the other focused on the southeastern section (Umhoefer and Schiarizza, 1996), the leading contractional end of the ripout structure. Combining the work from both papers links the Tchaikizan fault to the Marshall Creek fault

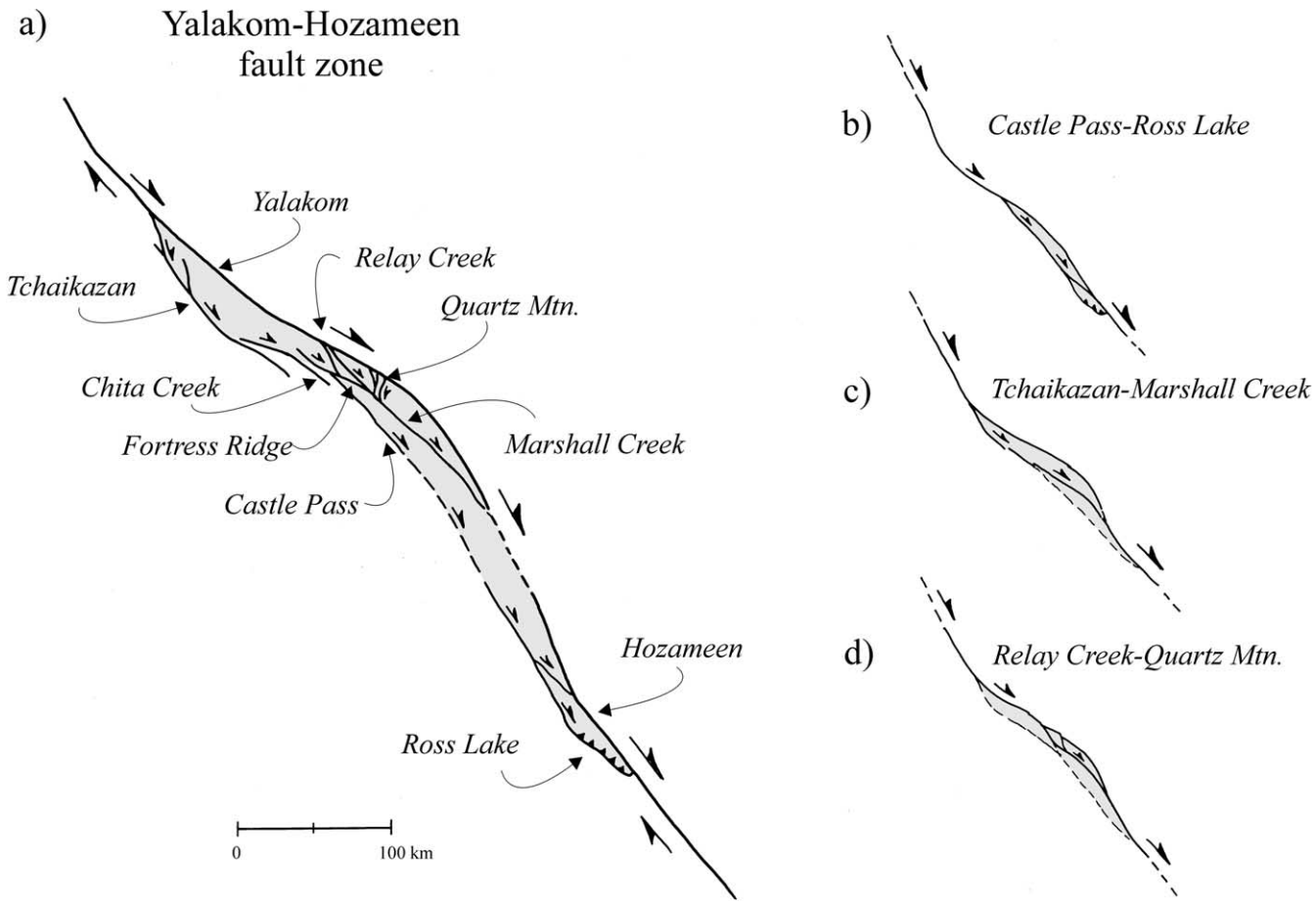

Fig. 8. Possible sidewall ripout structure in the Yalakom–Hozameen dextral strike-slip fault through southern British Columbia and Washington based on work by Umhoefer and Kleinspehn (1995), Umhoefer and Schiarizza (1996) and Miller (1994). (a) Mid-crustal ripout structure is localized on a restraining bend section of the fault system and shows a flanking slab nearly 500 km long and 25 km wide with the asymmetric ripout geometry expected for dextral shear. (b)–(d) Possible sequence of ripout slab development from cross-cutting relations of Umhoefer and Schiarizza (1996).

to define the flanking fault of this 300-km-long ripout slab. The trailing end of the structure is dominated by the Tchaikazan fault zone and connects through en échelon segments to the southeast. The leading end of the structure is defined by the Marshall Creek fault. Further correlations to the southeast across the younger dextral Fraser fault to the Hozameen and Ross Lake faults (with its thrust interpretation appropriate for its position in the overall ripout structure; Miller and Bowring, 1990; Miller, 1994) could extend the ripout structure to a possible total length of nearly 500 km (Fig. 8).

Using the fault reconstruction proposed by Umhoefer and Schiarizza (1996) for the southeastern section of the Yalakom fault, a possible sequence of sidewall ripout structures emerges (Fig. 8b–d) where the restraining bend geometry of the main (Yalakom–Hozameen) fault zone is progressively modified by adhesive wear. An initial ripout (Fig. 8b) is defined by the Castle Pass–Ross Lake fault (Umhoefer and Schiarizza, 1996) followed by a second slab (Fig. 8c) defined by the Tchaikizan–Chita Creek, Fortress Ridge and Marshall Creek faults (Umhoefer and Kleinspehn, 1995). Smaller scale ripouts further modify the structure (Fig. 8d) along the Relay and Quartz Mountain faults that correlate to further motion on the Marshall Creek fault (Umhoefer and Schiarizza, 1996).

3.2. Active faults in the southeastern Tibetan plateau

Strike-slip faults in active tectonic areas worldwide develop specific geomorphic characteristics that can be related to the geometry and kinematic history along the fault. Typical pull-apart basins and positive flower structures represent these effects where localized on releasing and restraining steps or bends along the faults (Sylvester, 1988). However, certain fault splay basins, where the fault splay links back to the main fault trace in ripout geometry, can also be seen, for example, in recent mapping efforts in active faults of western China (Wang et al., 1998). Here, coupled trailing pull-apart basins and leading edge thrusts and uplifts are developed along the flanks of larger strike-slip faults.

3.2.1. The Anninghe fault and flanking Pliocene basin

Within the complex strike-slip fault arrays associated with collision in western China, the Anninghe fault zone develops as a restraining linkage between the Xianshuihe and the Zemuhe faults (fig. 8 in Wang et al., 1998). Smaller scale lensing along the restraining segment suggests ripout geometries with lenses 50–100 km long and 10 km wide. The flanking lens structures along the Anninghe fault display localized uplift due to thrusting at the leading edge and a Pliocene sedimentary basin within the trailing ramp end of the structure.

3.2.2. East Xiaojiang fault and Dongchuan basin

Multiple fault lenses 2–3 km wide and 30 km long along the northern end of the East Xiaojiang fault zone (fig. 18 in Wang et al., 1998) show similar ripout geometries. The Dongchuan basin occurs along this sinistral strike-slip fault zone (Fig. 9a), is localized at the trailing extensional end of the structure and filled with Pleistocene and Holocene sediments with normal faults oblique to the main fault trace. The multiple ramps at the contractional end of the structure suggest imbrication of the leading end of this fault sliver, exposing older Permian rocks due to uplift and subsequent erosion.

3.2.3. Qujiang fault and E'shan basin

A ripout occurs along the Qujiang fault zone (Fig. 9b), a NW–SE-trending dextral strike-slip fault possibly related to the Red River fault zone (Wang et al., 1998). The flanking E'shan basin (fig. 38 in Wang et al., 1998) is an elongate Quaternary basin on the north side of the dextral Qujiang fault that is bounded by a flanking parallel fault trace. This defines a fault slab that is nearly 20 km long and 3 km wide with ripout asymmetry. Wang et al. (1998) interpreted the E'shan basin to be the result of localized extension at the east end of this fault slab (Fig. 9c) and proposed that slip is being transferred into extension and shortening at either end of the basin in accord with ripout kinematics.

3.3. San Andreas fault zone, southern California

Ripout geometries on the crustal scale, complete with flanking basin/uplift systems, occur along the restraining Transverse Ranges section of the San Andreas fault zone of southern California (Powell et al., 1993). Dibblee (1968) considered these fault lens geometries in his four-level classification of regional structure for the southern San Andreas fault. His classification included 'individual faults', 'fault zones' composed of many individual faults, the 'fault system' of multiple fault zones and many individual faults, and "within the system: a fourth term is needed to designate a series or group of faults or strands that branch from and rejoin the San Andreas fault and within a strip as wide as 20 miles (~30 km) through the Transverse Ranges" (Dibblee, 1968). He included the San Gabriel, Punchbowl and Banning fault zones in this special category. Fig. 10 shows several ripout geometries on a number of scales, the most distinctive being the proposed ripout formed by the 150-km-long San Gabriel fault zone. Smaller ripout geometries are also apparent along the main strand of the

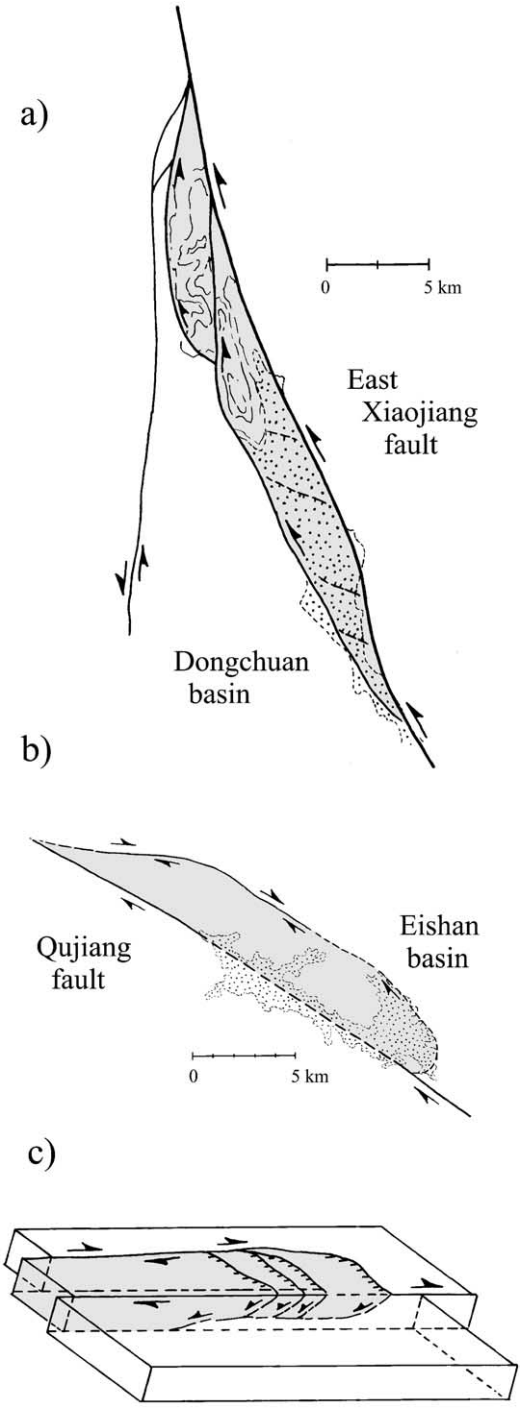

Fig. 9. Crustal-scale examples of ripout lenses from active faults in southeastern Tibet from Wang et al. (1998). (a) Multiple fault lenses along the East Xiaojiang fault zone showing the uplift topography coupled with a trailing Dongchuan sedimentary basin cut by oblique normal faults. (b) The Qujiang fault zone and a flanking ripout localize the E'shan basin at the trailing end of the interpreted structure. (c) Interpreted block diagram for basin formation. (Stippled pattern represents basin sedimentation).

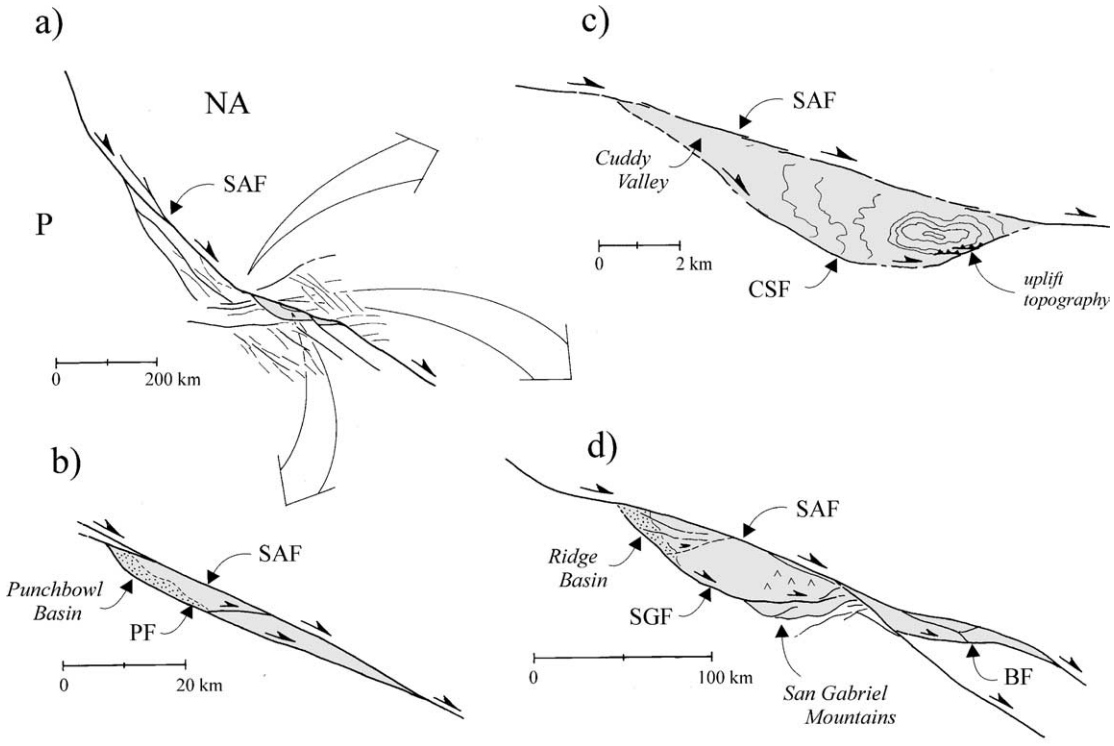

Fig. 10. Ripout geometries in the San Andreas fault zone. (a) The restraining bend and ripout lens geometry in the Transverse Ranges along the southern part of the San Andreas fault system (from Powell, 1993). (b) Geometry of the Punchbowl fault and the Punchbowl basin along the San Andreas fault zone within the larger San Gabriel structure (from Dibblee, 1968). (c) Smaller-scale ripout defined by the Cuddy Saddle fault from the western end of the Transverse Ranges as mapped by Davis and Duebendorfer (1987) with valley topography at the extensional end and uplift topography and minor thrusts at the leading end of the scallop-shaped structure. (d) Larger-scale San Gabriel/Banning ripout along the restraining Transverse Ranges segment of the San Andreas fault zone (from Powell, 1993). (BF: Banning fault; CSF: Cuddy Saddle fault; FF: Fenner fault; NA: North America; P: Pacific; PF: Punchbowl fault; SAF: San Andreas fault; SGF: San Gabriel fault; stippled pattern represents basin sedimentation).

San Andreas fault within the San Gabriel slab as seen in the geometry of the Punchbowl fault zone, 65 km long, defining a ripout slab 0.5 km wide associated with the trailing Punchbowl Basin (Fig. 10b). Fault geometries in the western end of the Transverse Ranges (Davis and Duebendorfer, 1987) include the Cuddy Saddle fault zone (Fig. 10c) that defines a 15-km-long ripout that lacks the typical asymmetry but includes localized zones of high and low topography at the leading and trailing ends of the structure.

3.3.1. The San Gabriel sidewall ripout

The San Gabriel fault splays off the main strand of the San Andreas and rejoins farther along strike to define an asymmetric plano-convex fault wall lens with ripout asymmetry, 150 km long and 30 km wide. This dextral asymmetry includes the trailing Ridge Basin and leading San Gabriel Mountain uplift (Fig. 10a and d). Interpretations by previous researchers (Fig. 11) all show part of this dextral ripout geometry in their San Gabriel reconstructions.

The restraining segment of the early San Andreas fault through the Transverse Ranges developed from 18–13 my during the early to middle Miocene and accommodated up to 110 km of displacement (Powell, 1993) prior to regional lock-up and the development of the San Gabriel fault. Most models for the development of the San Gabriel fault zone (Matti and Morton, 1993; Powell, 1993; Weldon et al., 1993) show that the San Gabriel was the principal displacement strand of the San Andreas system (Fig. 11a, for example) through this area for the L. Miocene–E. Pliocene. Movement on the San Gabriel fault (Fig. 12d) began in the Late Miocene from 14 to 12 my (Crowell, 1982) and persisted until 4–5 my (Fig. 12c). The end of activity on the San Gabriel system during the Pliocene led to the establishment of the modern San Andreas (Fig. 12b) to effectively cut off the San Gabriel fault with ~85 km of additional displacement (Powell, 1993). The origin of the bulge geometry for the San Gabriel fault and its relationship to the early San Andreas fault has not been adequately addressed but fits well with a model for crustal-scale adhesive wear and a ripout origin for the San Gabriel fault. The restraining Transverse Ranges section of the early San Andreas fault was key in developing the initial adhesion or resistance to slip needed to form the flanking San Gabriel fault (Fig. 12d) and drive the southeastward translation of the San Gabriel slab as a plowing asperity (Fig. 12c).

Researchers have considered varied roles for the early San Andreas fault in the development of the San Gabriel fault (Fig. 11). Powell (1993), for example, shows a remnant of this early San Andreas fault zone preserved as the San

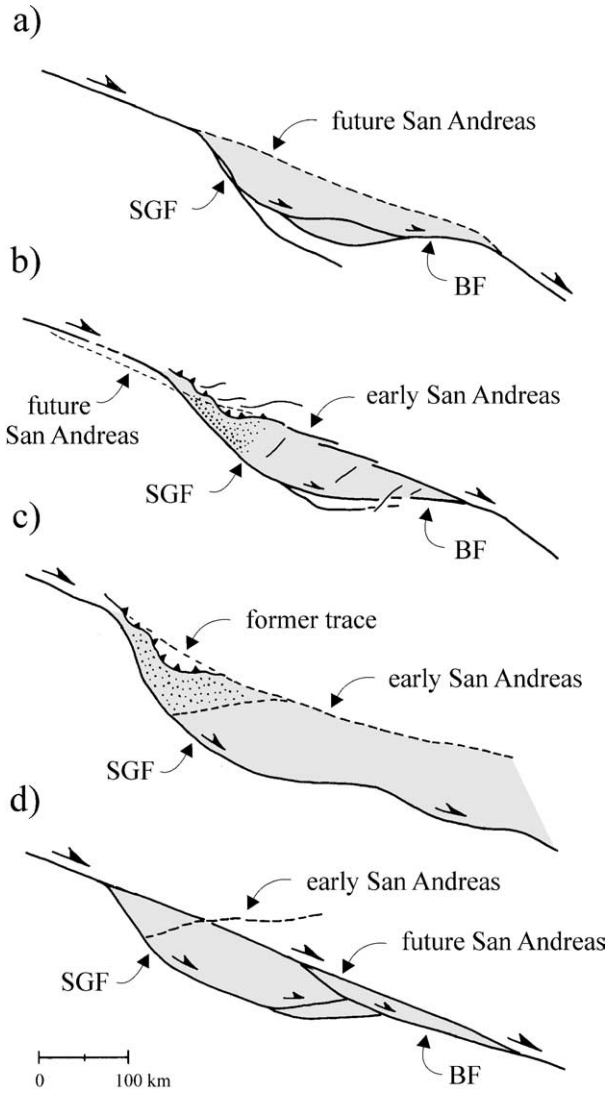

Fig. 11. Previously proposed Late Miocene reconstructions for the San Gabriel fault based on present day fault geometries and paleogeographic reconstructions. (a) San Gabriel transform system (after Powell, 1993) prior to the development of the future or modern San Andreas defines an indenting asperity geometry. (b) Weldon et al. (1993) show an equivalent geometry linking the San Gabriel to the Banning fault and show a possible trace for the early San Andreas fault that played a role in adhesion and ripout development. (c) Matti and Morton (1993) show the trace of the early San Andreas after San Gabriel displacement where it is preserved within the San Gabriel block as the early San Francisquito fault zone. (d) Crustal block reconstruction by Dillon and Ehlig (1993) showing the positions of the major faults and their asymmetric ripout geometry. (BF: Banning fault; SF: San Francisquito fault; SGF: San Gabriel fault; stippled pattern represents basin sedimentation).

Francisquito fault within the San Gabriel slab, now rotated and displaced along the San Gabriel fault. Weldon et al. (1993) proposed a 6–10 my movement history for the San Gabriel fault (Fig. 11b) with alternative early Miocene reconstructions, one of which used an early preexisting San Andreas. Matti and Morton (1993), as well as Dillon and Ehlig (1993), show the early San Andreas fault as the Francisquito–Fenner–Clemens Wells fault zone now displaced by the later western part of the San Gabriel fault (Fig. 11c and d). The Clemens Wells fault in these interpretations represents the eastern end of the early San Andreas but now occurs ~100 km to the southeast due to displacement along the modern San Andreas (Fig. 12b and c).

3.3.2. Trailing edge structures

The trailing extensional northwest end of the San Gabriel ripout (Figs. 10d, 11b and c and 12a) hosts a pull-apart structure, with fault-controlled sedimentation of the Violin breccia in the Late Miocene-age Ridge Basin (Crowell, 1982) that flanks the trace of the San Gabriel fault. The Ridge Basin has been modeled by Crowell (1982) as being caused by strike-slip motion along the San Andreas–San Gabriel fault zone transition with crustal block movement past a local obstructing bend that developed extensional strike-slip basins. The northern crustal block was thought to have pulled apart at a hypothesized 'asperity' formed at the intersection of the San Gabriel and the San Andreas faults. May et al. (1993) reinterpreted the basin in relation to strike-slip fault motion forming at a releasing bend in the system where dextral slip along the San Andreas fault was transferred to the SW side of the fault along the San Gabriel fault. This is similar to typical pull-apart basin formation (Mann et al., 1983) but the flanking fault rejoins the main fault farther along strike to complete the ripout geometry. The interpreted structure of May et al. (1993) shows a trailing extensional ramp with a flat-bottomed geometry defined by a flat lying detachment at nearly 4 km in depth similar to the model proposed for the E'shan basin of western China (Fig. 9c) as described above (Wang et al., 1998). Both of these structures can be interpreted as trailing pull-apart basins related to ripout translation.

The series of faults that cut obliquely across the northern end of the flanking San Gabriel slab (Fig. 12) are arranged chronologically from the older San Francisquito in the southeast to the younger Clearwater and to the even younger Liebre fault toward the northwest as the San Andreas is approached. Link (1982) and Crowell (1982) report that the Clearwater fault was active during the early part of Ridge

Fig. 12. Early Miocene to Present Day reconstruction of the San Gabriel ripout. (a) Present Day fault configuration in the Transverse Ranges (after Powell, 1993) including both San Gabriel and Banning fault lenses (b) Removal of 24 km of displacement from along the San Jacinto fault zone realigns the San Gabriel and Banning faults and better defines the tapered leading edge of a possible ripout structure that is nearly 200 km long and 30 km wide. The modern San Andreas fault represents a cutoff structure for the San Gabriel ripout asperity with ~85 km displacement of the Clemens Wells section of the early San Andreas fault. (c) The pre-modern San Andreas reconstruction represents the San Gabriel ripout translation and its history of soft-asperity plowing during continued adhesion with the 'half-graben' geometry of the trailing end and the 'humpback' geometry of the leading end of the ripout structure. (d) Initiation

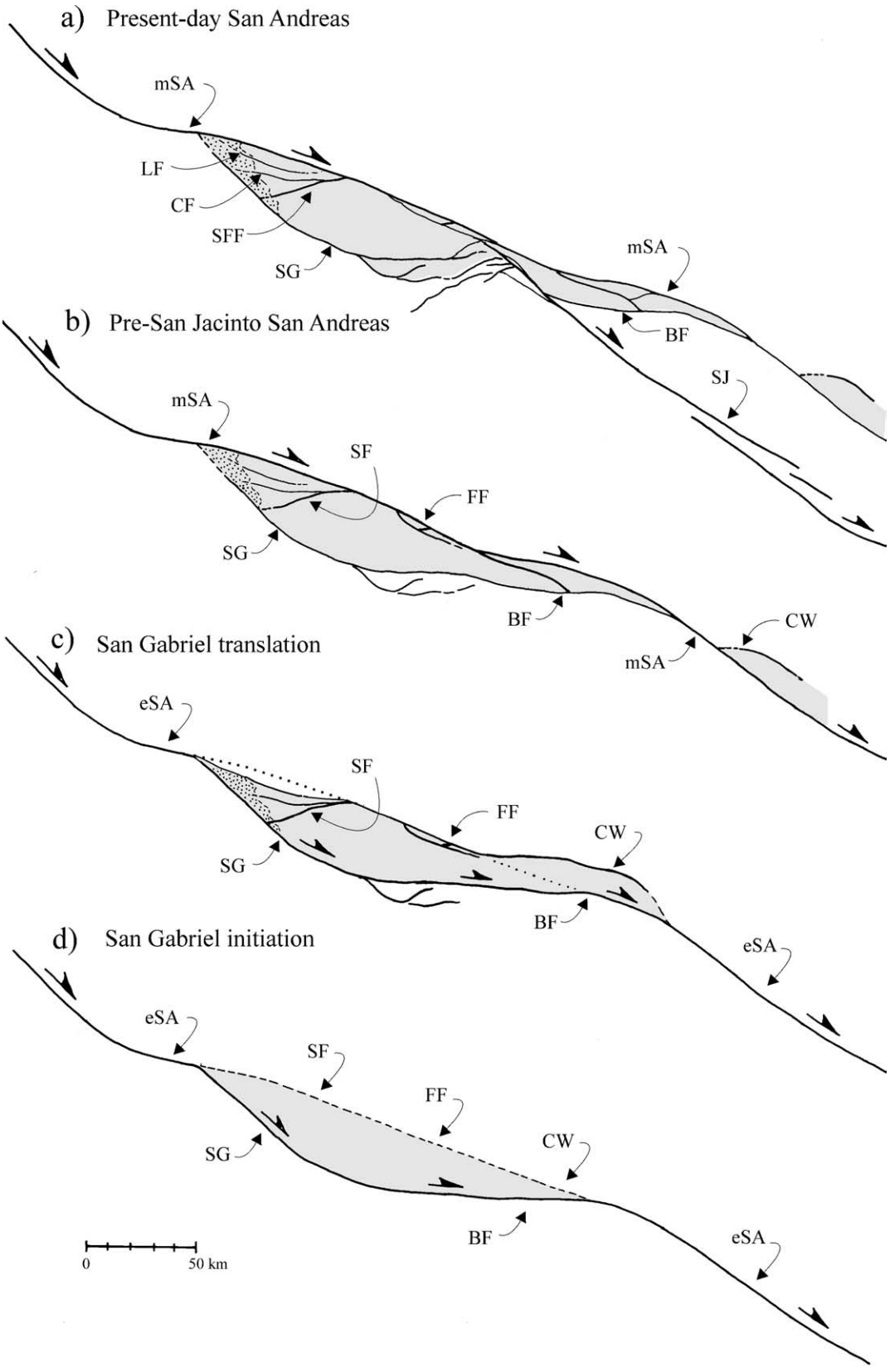

geometry of the San Gabriel/Banning ripout structure along the Transverse Ranges restraining segment of the San Andreas fault zone. (BF: Banning fault; CF: Clearwater fault; CW: Clemens Wells fault; FF: Fenner fault; LF: Liebre fault; eSA: early San Andreas fault; mSA: modern San Andreas fault; SG: San Gabriel fault; SFF: San Francisquito fault; SJ: San Jacinto fault; stippled pattern represents basin sedimentation; dashed line in (d) inactive section of the early San Andreas fault; dotted line in (c) represents the original position of the early San Andreas fault).

Basin formation with an estimated 3–4 km right-lateral slip component at around 8 my (Ensley and Verosub, 1982). The Liebre fault was active during Ridge Basin formation with 6.5 km of estimated right-lateral slip along two branches that were active sequentially with the older southern branch from 6 to 7 my and the northern branch from 5 to 6 my. Crowell (1982) also identified at least four Liebre fault segments that were overlapped by successively younger beds documenting the northeastern migration of the principal zone of movement during the time of Ridge Basin formation. What is proposed here is not the "north-northeastern migration of fault activity" (Crowell, 1982) but the progressive southerly migration of each inactivated fault section from astride the main trace of the San Andreas during translation of the San Gabriel block in a soft asperity plowing model (Fig. 4b). The San Francisquito, the Clearwater and finally the Liebre fault zones were, then, once-active strands of the main San Andreas fault that were rotated and displaced by slip along the San Gabriel fault. This suggests intermittent adhesion on the early San Andreas where reactivation of the main San Andreas would cut through anew along the original alignment and leave the abandoned earlier fault section displaced, rotated and preserved within the trailing end of the ripout slab (Fig. 12).

3.3.3. Leading edge structures

As the San Gabriel fault is followed to the southeast as a flanking strike-slip fault (Fig. 12), the trend of this fault swings back to rejoin the San Andreas fault through a series of oblique thrust or reverse fault zones that define the leading edge of the San Gabriel ripout slab and localize the related uplift in the San Gabriel Mountains. The leading contractional southeast end of the structure connects through a series of splays (Powell, 1993) such as the Canton and Vasquez Creek faults, high angle reverse faults of the northern and southern strands of the San Gabriel and the Sierra Madre and Cucamonga faults localizing uplift of the San Gabriel Mountains. The San Gabriel fault itself is thought to record 60–42 km of dextral displacement at its northwestern end associated with the Ridge Basin (Crowell, 1982; Powell, 1993) and lower displacement values at the southeast branches of the fault as other splays and thrusts help to accommodate the overall translation.

In the pre-San Jacinto fault reconstruction (Fig. 12b) the correlation of the San Gabriel and Banning faults (Fig. 11a, b and d) across the more recent San Jacinto fault zone as suggested by numerous workers (e.g. Powell, 1993; Weldon et al., 1993) makes possible a ripout structure that is nearly 200 km long. The reconstruction shown in Fig. 12b has removed the 24 km of right lateral displacement on the San Jacinto and realigns the San Gabriel and Banner fault zones to better define the leading contractional end of the ripout.

Continued adhesion and translation of the ripout slab along this leading ramp would lead to surface uplift and the formation of multiple ramps as in the hard-asperity plowing model (Fig. 4a). Movement on the leading ramp could also force the deformation of the adjacent wall rock (and the locked and abandoned part of the main fault zone) into the 'humpback' geometry (Fig. 12c) of the soft-asperity plowing model (Fig. 4b). The 'humpback' geometry of the inactive main fault produced by this mechanism represents an obstruction to any renewed displacement on the main fault zone. The main modern San Andreas fault may have developed as a 'humpback' cutoff along the former straight trace of the main fault to displace the Clemens Wells portion of the inactive main fault to its present day position (Fig. 12b).

4. Discussion

4.1. Three-dimensional geometry

The analysis of ripout structures thus far is based on two-dimensional plan views of the mapped faults. In the three-dimensional view these adhesive wear ripouts would form an ovoid patch or panel shape on the flanks of the main fault surfaces. The possible plan views through the adhesive wear panel for different levels of exposure vary from the downward converging faults of a lower 'keel' structure to the upwardly converging faults of an upper 'crest' structure. Plan view exposures through the center of an adhesive wear panel would have vertical flanking faults and vertical lateral ramps.

The across-strike cross-section geometry expected for most of the active near-surface fault zones would represent the downward converging keel structure for the bottom half of the adhesive wear panel. Shallow crustal scale features may also develop in widely-flaring, flat-bottomed keel geometry as seen in seismic reflection studies in the Ridge Basin and San Gabriel fault system (May et al., 1993). This keel structure is most commonly expressed as the upwardly flaring 'flower structure' described in numerous strike-slip fault studies (Sylvester, 1988). The typical positive flower structures for strike-slip faults can be interpreted as a product of adhesive wear due to strain hardening at restraining bends. Lock up along restraining fault sections will cut out petal-shaped crustal slabs (or ripouts) that can be shunted along the fault zone. This suggests that smaller pockets of extension can develop at the trailing ends of adhering crustal 'petals' within these positive flower structures.

4.2. Structural patterns

The adhesive wear process can introduce new geometric complexities into faults that have already evolved to a through-going fault zone. Continued displacement forces the evolving fault to become streamlined by adhesive wear and ripout formation at restraining bends and linkages. Multiple adhesion–reactivation sequences at either the

trailing or leading edges can introduce complex geometries. These new ripout complexities can increase the width of the fault zones, enhance bulk cataclastic flow and facilitate larger-scale fault zone development. Late stage adhesive wear offers a mechanism to introduce new structural complexities such as pull-apart basins in mature established fault zones as shown by Barnes et al. (2001) for the off-shore Alpine Fault zone in New Zealand.

The adhesive wear model also represents a likely pattern of fault zone deformation that can be used to better understand the complex structure within many exposed fault systems. The principles of adhesive wear can be used to aid in the reconstruction of crustal-scale tectonic boundaries. For example, regional tectonic models for the full San Andreas system by Sedlock and Hamilton (1991) portray the inception of the early San Andreas as part of the 'inboard' fault system that developed as the major offshore plate boundary began cutting out slightly arcuate lenses in the North American plate (Fig. 13a). Each lens-shaped cutout resembles the ripout structures described here and can be attributed to increased drag on the major outboard boundary as the transform system lengthened with continued ridge subduction and triple junction migration. In the 18 my reconstruction shown in Fig. 13b, Sedlock and Hamilton (1991) noted the apparent transpressional and transtensional nature of the different inboard fault zones in a distribution expected for dextral ripout structures. The net result is a significant widening of the plate boundary zone along the edge of the continental plate and the development of many crustal sheets or flakes (Sedlock and Hamilton, 1991) that can be better understood through the crustal-scale processes of adhesive wear.

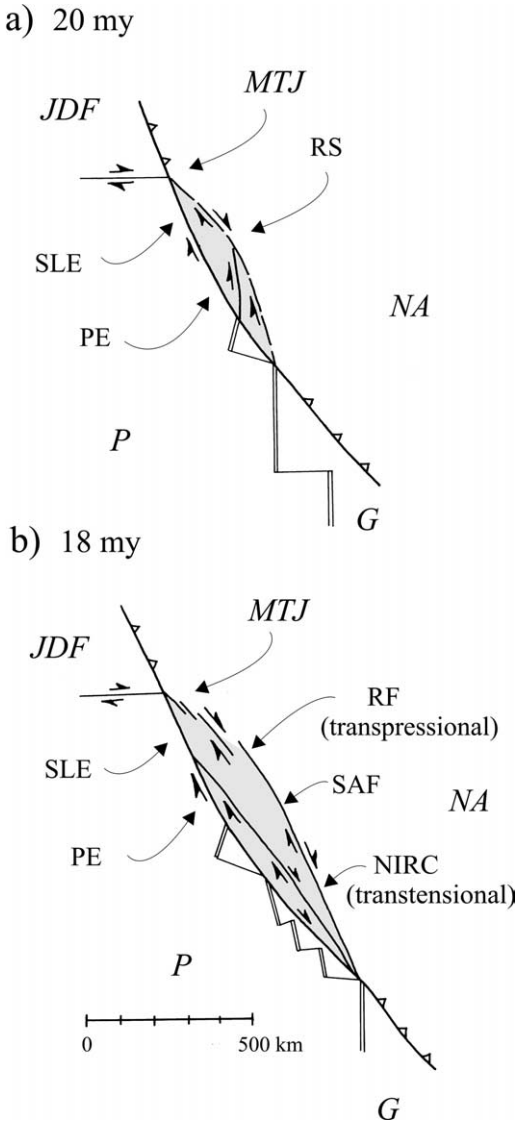

Fig. 13. The development of the San Andreas fault zone by crustal-scale adhesive wear during early transform history along the Santa Lucia and Patton escarpments at the edge of the continental plate. (a) and (b) Initiation of the 'inboard' dextral fault system as a step-wise process that cuts arcuate lenses (ripouts) out of the edge of the North American plate (modified after Sedlock and Hamilton, 1991). (G: Guadalupe plate; JDF: Juan de Fuca plate; MTJ: Mendicino triple junction; NA: North American plate; NIRC: Newport–Inglewood–Rose Canyon fault; P: Pacific plate; PE: Patton escarpment; RS: Russell fault; RF: Rinconada fault; SAF: San Andreas fault; SLE: San Lucia escarpment).

5. Conclusions

The abundance and distribution of sidewall ripouts within strike-slip fault zones suggest that adhesive wear was a significant deformation mechanism, particularly on sections of faults with restraining orientations. Ripout formation along restraining P-shear linkages between initial en échelon R-shears helps to accommodate displacement and modify the along strike geometry to produce a more uniform through-going fault zone. Continued displacement and localized adhesion along the interconnected system contributes to the residual lens geometry of mature fault zones and results in an anastomosing zone of bulk cataclastic flow.

Adhesive wear also involves material transfer across the main fault trace by shifting the zone of active faulting in the formation of the flanking fault and ripout structure. The resulting ripout geometry creates an effective asperity along the trace of the main fault that is forced to plow through the adjoining wall rock. This sets up the structural asymmetry, with contractional structures in front of the ripout/asperity and extensional structures behind the ripout/asperity during translation and plowing. A hard-asperity plowing model maintains the main fault trace with wall rock imbrication and extensional fracturing. A soft-asperity plowing model results in the rotation of the main fault trace in the trailing extensional end of the structure and the 'humpback' distortion of the main fault trace at the leading contractional end of the ripout. Multiple adhesion–reactivation sequences can led to complex internal fault relationships related to this structural asymmetry.

In active tectonic areas, crustal-scale adhesive wear is

expressed as a basin/uplift system localized along the flank of a larger strike-slip fault zone. Crustal ripouts occur up to 500 km long and 25–30 km wide. In these fault-bounded slabs and lenses the trailing extensional ramps are developed as strike-slip basins and the leading contractional ramps develop imbricate thrusts with associated uplift and erosion. An accurate model for outcrop- to crustal-scale adhesive wear aids in the interpretation of fault geometry and, when combined with linkage-growth for fault zone evolution from initially en échelon arrays, gives a more comprehensive strategy for fault zone reconstruction and kinematic analysis, particularly in interpreting deformation at restraining bends on strike-slip faults.

Acknowledgements

This research was supported by the U.S. Geological Survey's National Earthquake Hazards Reduction Program (NEHRP) through grants in 1985, 1987, 1989 and 1991 for work on detailed mapping of the dextral strike-slip fault zones of Cape Elizabeth, Maine. Thanks to Leo Algeo for assistance in plane-table-alidade mapping at Richmond Island, while an undergraduate student at the University of Southern Maine and to Tom Blenkinsop and David Peacock as reviewers who helped to improve the manuscript.

References

Arriagada, C., Roperch, P., Mpodozis, C., 2000. Clockwise block rotation along the eastern border of the Cordillera de Domeyko, Northern Chile (22°45′–23°30′S). Tectonophysics 326, 153–171.

Barnes, P.P., Sutherland, R., Davy, B., Delteil, J., 2001. Rapid creation and destruction of sedimentary basins on mature strike-slip faults: an example from the offshore Alpine Fault, New Zealand. Journal of Structural Geology 23, 1727–1739.

Bartlett, W.L., Friedman, M., Logan, J.M., 1981. Experimental folding and fracturing of rocks under confining pressure. Part IX. Wrench faults in limestone layers. Tectonophysics 79, 255–277.

Bowden, F.P., Taber, D., 1973. Friction—An Introduction to Tribology. Anchor Press, Doubleday, New York.

Bowman, W.F., Stachowiak, G.W., 1996. A review of scuffing models. Tribology Letters 2, 113–131.

Brown, M., Diaz, F., Grocott, J., 1993. Displacement history of the Atacama fault system 25°00′S–27°00′S, northern Chile. Geological Society of America Bulletin 105, 1165–1174.

Crowell, J.C., 1982. The tectonics of the Ridge Basin, southern California. In: Crowell, J.C., Link, M.H. (Eds.), Geologic History of Ridge Basin, Southern California Pacific Section Society of Economic Paleontologists and Mineralogists, pp. 25–41.

Curtis, M.L., 1999. Structural and kinematic evolution of a Miocene to Recent sinistral restraining bend: the Montejunto Massif Portugal. Journal of Structural Geology 21, 39–54.

Davis, G.H., Reynolds, S.J., 1996. Structural Geology of Rocks and Region, 2nd edition J. Wiley & Sons. 776pp.

Davis, T.L., Duebendorfer, E.M., 1987. Strip map of the western big bend segment of the San Andreas fault. Geological Society of America, Map & Chart Series MC-60.

Dibblee Jr., T.W., 1968. Displacements on the San Andreas fault system in the San Gabriel, San Bernadino and San Jacinto Mountains, southern California. In: Dickinson, W.A., Grantz, A. (Eds.), Proceedings of a Conference on Geologic Problems of the San Andreas Fault System California Stanford University Publications in Geological Sciences, 11, pp. 260–276.

Dillon, J.T., Ehlig, P.L., 1993. Displacement on the southern San Andreas fault. In: Powell, R.E., Weldon II., R.J., Matti, J.C. (Eds.), The San Andreas Fault System: Displacement, Palinspastic Reconstruction, and Geologic Evolution Geological Society of America, Boulder, CO, Memoir, 178, pp. 199–216.

DiToro, G., Pennachioni, G., 2004. Superheated friction-induced melts in zoned pseudotachylytes within the Adamello tonalites (Italian Southern Alps). Journal of Structural Geology 26, 1783–1801.

Ensley, R.A., Verosub, K.L., 1982. Biostratigraphy and magnetostratigraphy of southern Ridge basin, central Transverse Ranges. In: Crowell, J.C., Link, M.H. (Eds.), Geologic History of Ridge Basin, Southern California Society of Economic Paleontologists & Mineralogists, pp. 13–24.

Grocott, J., 1981. Fracture geometry of pseudotachylyte generation zones: a study of shear fractures formed during seismic events. Journal of Structural Geology 3, 169–178.

Hancock, P.L., Barka, A.A., 1987. Kinematic indicators on active normal faults. Journal of Structural Geology 9, 573–584.

Link, M.H., 1982. Provenance, paleocurrents, and paleogeography of Ridge Basin, Southern California. In: Crowell, J.C., Link, M.H. (Eds.), Geologic History of Ridge Basin, Southern California Pacific Section, Society of Economic Paleontologists and Mineralogists, pp. 265–276.

Mann, P., Hempton, M.R., Bradley, D.C., Burke, K., 1983. Development of pull-apart basins. Journal of Geology 91, 529–554.

Marsh, A.J., Pachan, D.S., Sims, D.W., 1990. Strike-slip duplexing: an analog model for transpressional plate margins. Geological Society of America, Abstracts with Programs 22, 143A.

Matti, J.C., Morton, D.M., 1993. Paleogeographic evolution of the San Andreas fault in southern California: a reconstruction based on a new cross-fault correlation. In: Powell, R.E., Weldon II., R.J., Matti, J.C. (Eds.), The San Andreas Fault System: Displacement, Palinspastic Reconstruction, and Geologic Evolution Geological Society of America, Boulder, CO, Memoir, 178, pp. 107–160. Plate III-A and III-B.

May, S.R., Ehman, K.D., Gray, G.G., Crowell, J.C., 1993. A new angle on the tectonic evolution of the Ridge Basin, a 'strike-slip' basin in southern California. Geological Society of America Bulletin 105, 1357–1372.

Miller, R.B., 1994. A mid-crustal contractional stepover zone in a major strike-slip system, North Cascades, Washington. Journal of Structural Geology 16, 47–60.

Miller, R.B., Bowring, S.A., 1990. Structure and chronology of the Oval Peak batholith and adjacent rocks: implications for the Ross Lake fault zone, North Cascades, Washington. Geological Society of America Bulletin 102, 1361–1377.

Naylor, M.A., Mandl, G., Sijpesteijn, C.H.K., 1986. Fault geometries in basement induced wrench faulting under different initial stress states. Journal of Structural Geology 8, 737–752.

Petit, J.P., 1987. Criteria for the sense of movement on fault surfaces in brittle rocks. Journal of Structural Geology 9, 597–608.

Powell, R.E., 1993. Balanced palinspastic reconstruction of pre-late Cenozoic paleogeography, southern California: geologic and kinematic constraints on evolution of the San Andreas Fault system. In: Powell, R.E., Weldon II., R.J., Matti, J.C. (Eds.), The San Andreas Fault System: Displacement, Palinspastic Reconstruction, and Geologic Evolution Geological Society of America, Boulder, CO, Memoir, 178, pp. 1–106. Plate I.

Powell, R.E., Weldon II., R.J., Matti, J.C., 1993. The San Andreas Fault System: Displacement, Palinspastic Reconstruction, and Geologic Evolution, 178 Geological Society of America Memoir, Boulder, CO. 332pp.

Rabinowicz, E., 1965. Friction and Wear in Materials. John Wiley, New York.

Reijs, J., McClay, K., 1998. Salar Grande pull-apart basin, Atacama Fault System, northern Chile. In: Holdsworth, R.E., Strachan, R.A., Dewey, J.F. (Eds.), Continental Transpressional and Transtensional Tectonics Geological Society of London, Special Publications, 135, pp. 127–141.

Riecker, R.E., 1965. Fault plane features, an alternative explanation. Journal of Sedimentary Petrology 35, 746–748.

Samuels, L.E., Doyle, E.D., Turley, D.M., 1981. Sliding wear mechanisms. In: Rigney, D.A. (Ed.), Fundamentals of Friction and Wear of Materials, ASM Materials Science Seminar. American Society of Metals, Metals Park, Ohio, pp. 13–41.

Sedlock, R.L., Hamilton, D.H., 1991. Tectonic evolution of southwestern California. Journal of Geophysical Research 96, 2325–2351.

Swanson, M.T., 1988. Pseudotachylyte-bearing strike-slip duplex structures in the Fort Foster Brittle Zone, S. Maine. Journal of Structural Geology 10, 813–828.

Swanson, M.T., 1989. Sidewall ripouts in strike-slip faults. Journal of Structural Geology 11, 933–948.

Swanson, M.T., 1999. Dextral transpression at the Casco Bay restraining bend, Norumbega fault zone, coastal Maine. In: Ludman, A., West Jr., D.P. (Eds.), Norumbega Fault System of the Northern Appalachians Boulder CO, Geological Society of America Special Paper, 331, pp. 85–104.

Sylvester, A.G., 1988. Strike-slip faults. Geological Society of America Bulletin 100, 1666–1703.

Taylor, G.K., Grocott, J., Pope, A., Randall, D.E., 1998. Mesozoic fault systems, deformation and fault block rotation in the Andean forearc: a crustal scale strike-slip duplex in the Coastal Cordillera of northern Chile. Tectonophysics 299, 93–109.

Tchalenko, J.S., 1970. Similarities between shear zones of different magnitudes. Geological Society of America Bulletin 81, 1625–1640.

Theunnissen, K., Smirnova, L., Dehandschutter, B., 2002. Pseudotachylytes in the southern border fault of the Cenozoic intracontinental Teletsk basin (Altai, Russia). Tectonophysics 351, 169–180.

Tija, H.D., 1967. Sense of fault displacements. Geologie en Mijnbouw 46, 392–396.

Tija, H.D., 1968. Fault plane markings. Proceedings of the 23rd International Geologic Congress 13, 279–284.

Tija, H.D., 1971. Fault movement, reoriented stress field and subsidiary structures. Pacific Geology 5, 49–70.

Umhoefer, P.J., Kleinspehn, K.L., 1995. Mesoscale and regional kinematics of the northwestern Yalakom fault system: major Paleogene dextral faulting in British Columbia, Canada. Tectonics 14, 78–94.

Umhoefer, P.J., Schiarizza, P., 1996. Latest Cretaceous to early Tertiary dextral strike-slip faulting on the southeastern Yalakom fault system, southeastern Coast Belt, British Columbia. Geological Society of America Bulletin 108, 768–785.

Vingsbo, O., Hogmark, S., 1981. Wear of steels. In: Rigney, D.A. (Ed.), Fundamentals of Friction and Wear of Materials, ASM Materials Science Seminar. American Society of Metals, Metals Park, Ohio, pp. 373–408.

Walsh, J.J., Waterson, J., Bailey, W.R., Childs, C., 1999. Fault relays, bends and branchlines. Journal of Structural Geology 21, 1019–1026.

Wang, B.C., Burchfiel, L.H., Royden, L.H., Chen, L., Liangzhong, C., Jishen, C., Wenxin, L., 1998. Late Cenozoic Xianshuihe–Xiaojiang, Red River, and Dali fault systems of southwestern Sichuan and central Yunnan, China. Geological Society of America Special Paper 327 1998. 112pp.

Weldon, R.J., Meisling, K.E., Alexander, J., 1993. A speculative history of the San Andreas fault in the central Transverse ranges, California. In: Powell, R.E., Weldon II., R.J., Matti, J.C. (Eds.), The San Andreas Fault System: Displacement, Palinspastic reconstruction, and Geologic Evolution Geological Society of America, Boulder, CO, Memoir, 178, pp. 161–198.

Woodcock, N.H., Fischer, M., 1986. Strike-slip duplexes. Journal of Structural Geology 8, 725–735.

Woodcock, N.H., Schubert, C., 1995. Continental strike-slip tectonics. In: Hancock, P.L. (Ed.), Continental Deformation. Pergamon Press, Oxford, pp. 251–263.